

## Raman matrix isolation spectroscopy of dihydrogen. II. Aggregation processes in argon

M. E. Alikhani, L. Manceron, and J. P. Perchard

Citation: *The Journal of Chemical Physics* **92**, 22 (1990); doi: 10.1063/1.458468

View online: <http://dx.doi.org/10.1063/1.458468>

View Table of Contents: <http://scitation.aip.org/content/aip/journal/jcp/92/1?ver=pdfcov>

Published by the [AIP Publishing](#)

---

### Articles you may be interested in

[Ultrafast quantum dynamics and resonance Raman spectroscopy of photoexcited I2\(B\) in large argon and xenon clusters](#)

*J. Chem. Phys.* **104**, 9332 (1996); 10.1063/1.471678

[Optical Stark spectroscopy of molecular aggregates](#)

*J. Chem. Phys.* **104**, 5415 (1996); 10.1063/1.471781

[Cooperative effects in nonlinear optical spectroscopy of Jagggregates](#)

*AIP Conf. Proc.* **364**, 517 (1996); 10.1063/1.50167

[Laser Raman phonon spectroscopy of solid state photoreaction: Photodimerization of Omethoxy TRANS cinnamic acid](#)

*AIP Conf. Proc.* **160**, 580 (1987); 10.1063/1.36823

[Interferences in the Raman excitation profile for the intensity of normal modes of aggregated chlorophyll a](#)

*AIP Conf. Proc.* **160**, 571 (1987); 10.1063/1.36821

---



# Raman matrix isolation spectroscopy of dihydrogen. II. Aggregation processes in argon

M. E. Alikhani, L. Manceron, and J. P. Perchard

*Laboratoire de Spectrochimie Moléculaire (CNRS, UA 508) Université Pierre et Marie Curie, 4 Place Jussieu 75252 Paris Cedex 05, France*

(Received 24 May 1989; accepted 19 September 1989)

The vibrational spectra of  $\text{H}_2$ ,  $\text{D}_2$ , and HD trapped in solid argon were examined as a function of concentration and sample annealing. Before annealing, increasing the hydrogen concentration only leads to an asymmetrical broadening and a small blue shift of the  $Q(J)$  lines assigned to monomeric species. These observations are believed due to formation of low stoichiometry aggregates. After annealing above 35 K, new features— $10\text{ cm}^{-1}$  blue shifted with respect to monomer and small aggregate lines—appear with properties comparable to those reported for solid dihydrogen at 2 K. Force field calculations on aggregates involving two to six molecules (including ortho/para and isotopic mixtures) allow a semiquantitative interpretation of the experimental data, and suggest an aggregation degree larger than six. Finally it is concluded that a possible interpretation of all the data is the formation of microcrystals upon annealing, tied to the low solubility and the high mobility of dihydrogen in solid argon.

## INTRODUCTION

As a first part of a study devoted to the trapping of hydrogen in solid rare gases (Ref. 1, referred to as I), we have considered the Raman response of monomeric  $\text{H}_2$ , HD,  $\text{D}_2$  isotopic species isolated in Ar, Kr, and Xe. The vibrational spectra, recorded at 10 K just after deposition at the same temperature, displayed one (HD) or two ( $\text{H}_2$ ,  $\text{D}_2$ ) narrow lines assigned to  $Q_1(J)$  transitions of monomers; after warm up above 35 K, these signals decreased in intensity, with concomitant appearance of new lines at higher frequencies. Some of these lines had been previously reported by Prochaska and Andrews<sup>2</sup> and assigned to aggregates without further comments. However it appeared in the course of this study that information on the nature of these aggregates could be obtained from complementary experiments such as isotopic mixtures or variation of the ortho/para concentration ratio for  $\text{H}_2$  and  $\text{D}_2$ . Furthermore, some striking analogies with the Raman spectra of solid  $\text{H}_2$  and  $\text{D}_2$  reported by Welsh's group<sup>3,4</sup> were noted, giving support to the interpretation of matrix data. Finally, we have reexamined in detail the aggregation process in solid argon and the purpose of this paper is to describe in a first part the spectral data relating to  $\text{H}_2$ , HD, and  $\text{D}_2$  polymers in argon, and, in a second part, to discuss the nature of these polymers through force field calculations.

## EXPERIMENTAL

The vacuum system, cryostat, deposition, and spectral recording conditions have been described in I. Aggregates were obtained by cycling the sample temperature several times to 35–40 K. Temperature increase was performed at very slow rate, about  $1\text{ K min}^{-1}$ , in order to prevent fast boil-off of hydrogen and detachment of the sample from the sample holder. It was observed that thin samples, deposited with a gaseous mixture injection rate of 0.1 mmol per hour ( $\approx 30\text{ }\mu\text{mol/h}$  deposition rate from interference fringes

measurement) for about 15 h gave better results than thicker samples deposited at a rate two or three times faster. Indeed, thin samples show less tendency to crack, even after several annealing cycles up to 40–42 K. Rare gas/hydrogen gaseous mixtures were prepared with a hydrogen/Ar molar fraction of about 0.018 to 0.12. As shown in I, the  $\text{H}_2/\text{Ar}$  molar ratio of the matrix sample is about twice as low as that of the gaseous mixture, owing to the poor trapping efficiency of  $\text{H}_2$  at 10 K with respect to Ar, Kr, or Xe. These relative trapping efficiencies could be estimated and only the corrected values (ranging from 0.009 to 6.0) will be given in what follows. As in the case of monomers, each Raman line of hydrogen aggregates was recorded together with one neon emission line superimposed on the matrix spectrum during the same running scan.

## RESULTS

Results concerning experiments performed with HD will be reported first. For this molecule which exists at 10 K exclusively in the  $J = 0$  rotational state, the vibrational spectra are simpler than that of  $\text{H}_2$  and  $\text{D}_2$  molecules for which both  $J = 0$  and 1 levels are populated. These will be discussed in light of the results obtained for HD. This description will hinge on the observations made at variable ortho/para ratio for  $\text{H}_2$ . At last important results obtained for isotopic mixtures will be separately reported.

### HD/Ar

Experiments were carried out over a wide range of experimental conditions in order to investigate the roles of concentration and annealing on the state of aggregation of HD. A series of matrices was examined, with HD molar fraction varying between 0.009 and 0.03. The vibrational spectrum recorded at 9 K just after deposition displays one  $Q(0)$  line assigned in I to monomeric HD. The frequency and band profile of this line were seen to slightly vary with the HD

concentration. At low concentration ( $\text{HD}/\text{Ar} \leq 0.009$ ) the  $Q(0)$  line at  $3615.4 \text{ cm}^{-1}$  has a symmetrical profile with apparent full-width at half-maximum (FWHM) of  $0.9 \text{ cm}^{-1}$  (spectral slit width of  $0.8 \text{ cm}^{-1}$ ) while at  $\text{HD}/\text{Ar} = 0.03$ ,  $Q(0)$  is observed at  $3616.0 \text{ cm}^{-1}$  with an asymmetrical band profile and FWHM of  $1.1 \text{ cm}^{-1}$ . The band broadening mainly affects the high frequency side. As shown in Fig. 1, the effects of annealing depend both on temperature and sample concentration. Cycling the matrix temperature of a  $\text{HD}/\text{Ar} = 1/100$  sample to 38 K and then back to 10 K leads to the appearance of one additional weak band, hereafter referred to as  $P'$ , at  $3623.4 \text{ cm}^{-1}$  (Table I). After successive temperature cyclings up to 40–42 K the situation does not change significantly, except that the overall spectrum becomes weaker as more hydrogen boils off. For a HD concentration of 0.019, a short annealing to 38 K first leads to the appearance of the  $P'$  line with a rather strong intensity, with two low frequency shoulders at about  $3622$  ( $P$ ) and  $3620 \text{ cm}^{-1}$  ( $P''$ ). Successive annealings at increasing temperatures lead to intensity inversion between  $P$  and  $P'$ , and  $P'$  finally totally vanishes above 40 K. A systematic study of the  $P/P'$  formation and interconversion was performed in a narrow concentration range ( $\text{HD}/\text{Ar} = 0.009$  to  $0.03$ ) using in each case the same experimental procedure. In a first step the matrix temperature is slowly increased up to 38 K and then quickly lowered to 10 K; a spectrum was recorded, which defines the first step of migration-allowed

aggregation. Then, several annealing cycles are successively performed in the 38–42 K temperature range. Progressive spectral changes are observed until, finally, no more evolution is denoted. The last step defines the final state of aggregation. For annealing temperatures higher than 42 K, the samples become too scattering. Figure 2 displays the evolutions of the first and last steps of aggregation with respect to the  $\text{HD}/\text{Ar}$  molar ratio. The first step is always characterized by the predominance of  $P'$ , whose intensity with respect to the  $Q(0)$  monomer line strongly increases with the HD concentration. We have reported in Fig. 3 the dependence of the  $P'/Q(0)$  intensity ratio with the HD concentration on a logarithmic scale. This dependence is roughly linear, with a mean square regression slope of 2.1. The last step of aggregation also strongly differs according to the HD concentration. For  $\text{HD}/\text{Ar}$  molar ratios lower than 0.016,  $P'$  is predominant and  $P$  is scarcely observed; above this limit the situation is reversed since  $P'$  completely disappears at the benefit of  $P$  whose intensity strongly increases with respect to that of  $Q(0)$  when HD concentration increases (Fig. 1). Again, in the concentration range in which  $P$  is observed, one finds that the dependence of  $P/Q(0)$  intensity ratio with the HD concentration is roughly linear on a logarithmic scale, with a slope of about 7. Another remarkable observation is the dependence of the aggregate spectrum with the recording temperature. While the  $Q(0)$  line of HD monomer is very weakly blue shifted when the temperature of the sample is increased ( $\geq 0.5 \text{ cm}^{-1}$ ), the polymer bands experience a large blue shift (Fig. 4); furthermore there is a broadening of the main component so that the overall intensity seems to be

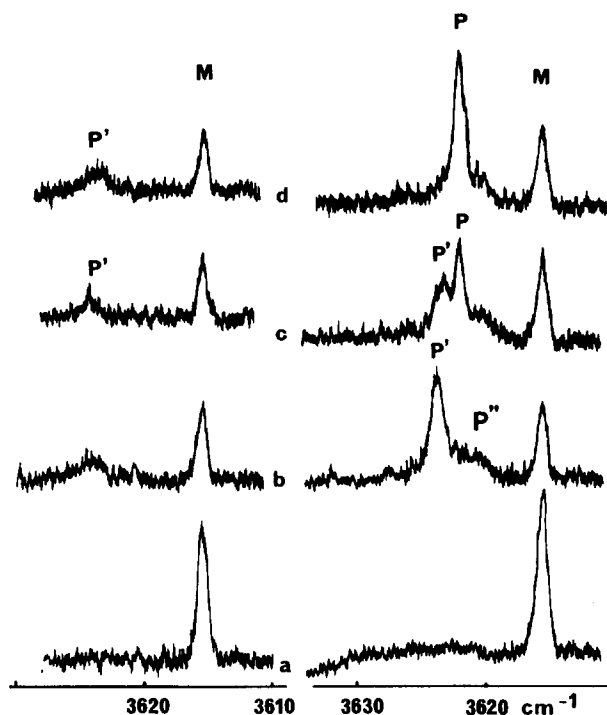


FIG. 1. Effect of the concentration on the spectral evolution of the  $Q$  branch of HD in solid argon for different annealing temperature. Spectra recorded at 10 K with spectral slit width of  $0.8 \text{ cm}^{-1}$ . Left:  $\text{HD}/\text{Ar} = 0.009$ ; right:  $\text{HD}/\text{Ar} = 0.019$ . (a) After deposition at 10 K at  $0.13 \text{ mmol/h}$  for 15 h. (b) After a first annealing to 38 K. (c) After a second annealing to 40 K. (d) After a third annealing to 42 K,  $M$  = monomer.  $P$ ,  $P'$ ,  $P''$  = polymer species.

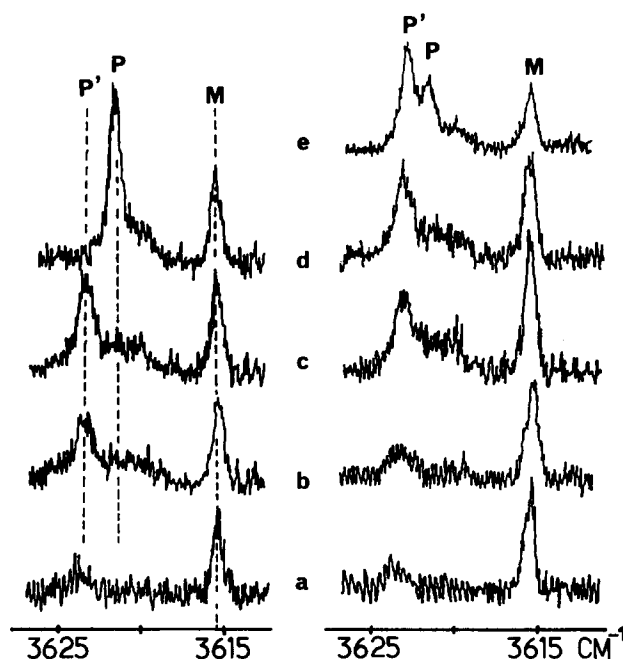


FIG. 2. Comparison of the initial (right) and final (left) states of aggregation of HD trapped in Ar as a function of the concentration. Spectra recorded at 10 K after annealing to 38 K (initial state) or after several annealings to 40–42 K (final state). Molar fractions in HD: (a) 0.009, (b) 0.013, (c) 0.016, (d) 0.019, (e) 0.030.

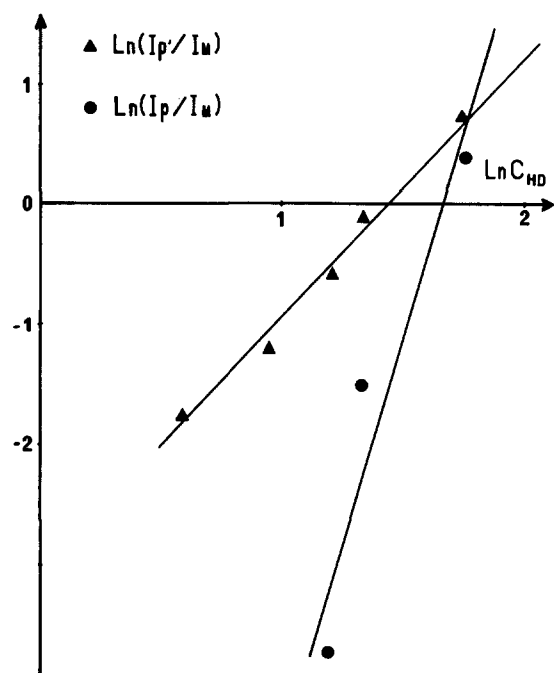


FIG. 3. Logarithmic plot of the intensity ratio of  $P$  and  $P'$  aggregates to monomer lines vs  $HD/Ar$  molar ratio (in mol%). Final observations made after annealing at 40 K (final state of aggregation).

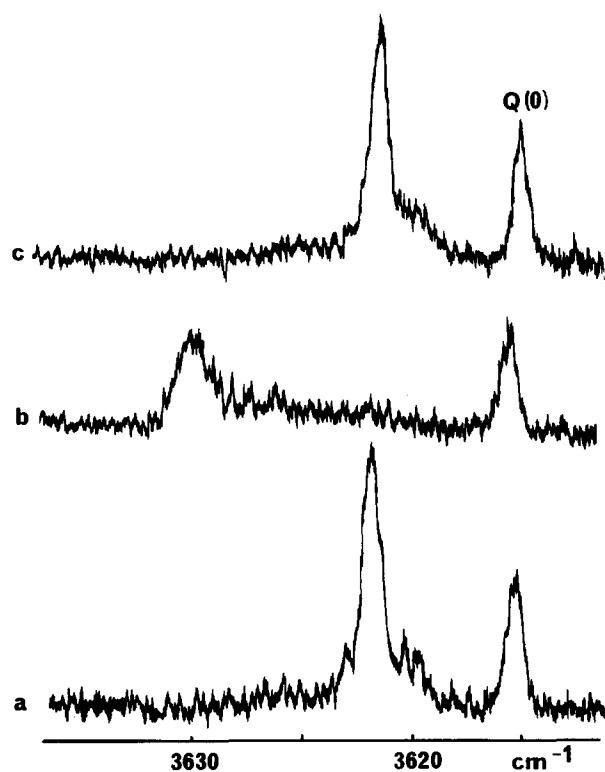


FIG. 4. Temperature dependence of the vibrational spectrum of HD trapped in solid  $Ar/HD/Ar = 0.019$ . Spectra successively recorded at different temperatures ( $T_r$ ) after annealing at 40 K. (a)  $T_r = 10$  K; (b)  $T_r = 38$  K; (c)  $T_r = 10$  K.

spread over the whole  $3620\text{--}3630\text{ cm}^{-1}$  range. The shift of the main line is found to be proportional to the temperature increase, with a rate of  $0.25\text{ cm}^{-1}\text{ K}^{-1}$ . These spectral changes are reversible, the lines recovering at low temperature their initial position and intensities as long as the temperature does not exceed 38 K.

## $H_2/Ar$

Concentration effects on the  $Q(0)$  and  $Q(1)$  lines of monomeric  $H_2$  was described in I. Both lines are slightly blue shifted in frequency as the  $H_2$  molar fraction increased (Table IV of I), with concomitant band broadening. Figure 5 shows the spectral evolution of a  $H_2/Ar = 2/100$  matrix upon annealing. The lower trace (spectrum recorded just after deposition) corresponds to monomeric  $H_2$ , with a  $Q(1)/Q(0)$  intensity ratio of 2.6 (3.0 in absence of ortho  $\rightarrow$  para conversion). Cycling the matrix temperature up to 38 K and then back to 10 K allows diffusion of the  $H_2$  molecules, leading to the appearance of new lines at  $4145.8$  and  $4152.7\text{ cm}^{-1}$ , with a relative intensity ratio of the order of 5. A second annealing to 40 K leads to a red shift of these polymeric lines which are now measured at  $4144.5$  and  $4151.5\text{ cm}^{-1}$ . According to the observations made for HD, the first doublet corresponds to species  $P'$ , and the second to  $P$ . Other experiments were carried out with variable ortho/

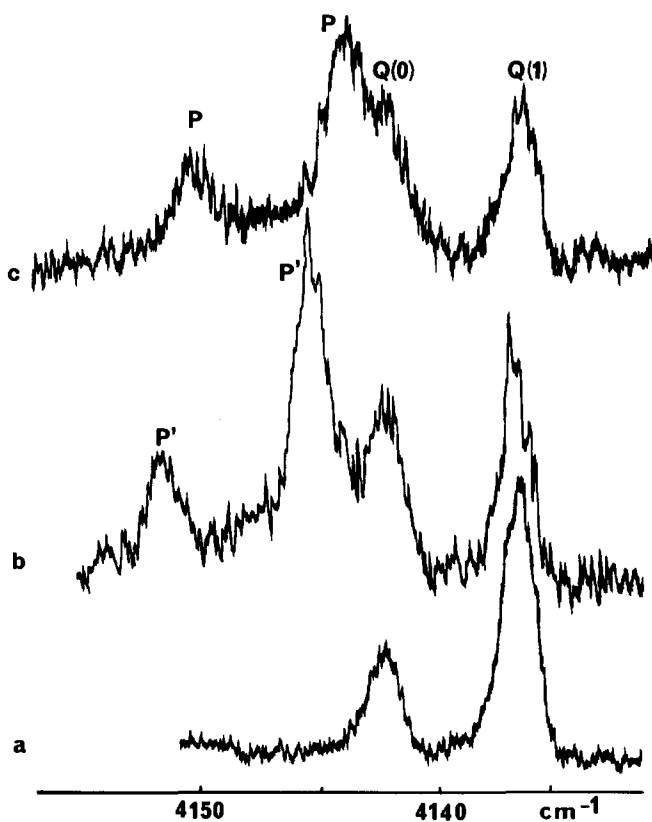


FIG. 5. Annealing effect on the vibrational spectrum of  $H_2$  trapped in solid  $Ar/H_2/Ar = 2/100$ . Recording temperature: 10 K. (a) after deposition at 10 K; (b) after a first annealing to 38 K; (c) after a second annealing to 40 K.

para molar ratios by introducing oxygen traces in the gaseous mixture before deposition. The two new bands observed after several temperature cycles to 38–40 K vary both in frequencies and relative intensities (Fig. 6) according to the following rules: for decreasing values of the ortho/para ratio, the low frequency component increases in frequency and decreases in intensity while the high frequency component decreases in frequency and increases in intensity.

### D<sub>2</sub>/Ar

As in the case of the other isotopic species, two steps of aggregation are identified during the successive annealing cycles. After cycling the matrix temperature of a D<sub>2</sub>/Ar = 2/100 sample to 38 K there appears a first doublet *P'* at 2986.9–2984.9 cm<sup>-1</sup>, with concomitant decrease of the *Q*(0)–*Q*(1) monomeric doublet at 2979.2–2977.0 cm<sup>-1</sup>. After a second annealing to 40 K, the *P'* doublet is replaced by the doublet *P* at 2985.1–2983.1 cm<sup>-1</sup>. Most strikingly in both *P'* and *P* doublets the intensity of the low frequency component is roughly three times greater than that of the high frequency one, in contrast with the value of the *Q*(1)/*Q*(0) intensity ratio of D<sub>2</sub> monomer, of the order of 0.4. Therefore the high and low frequency components of these doublets cannot be simply assigned to ortho and para D<sub>2</sub> molecules within two kinds of aggregates.

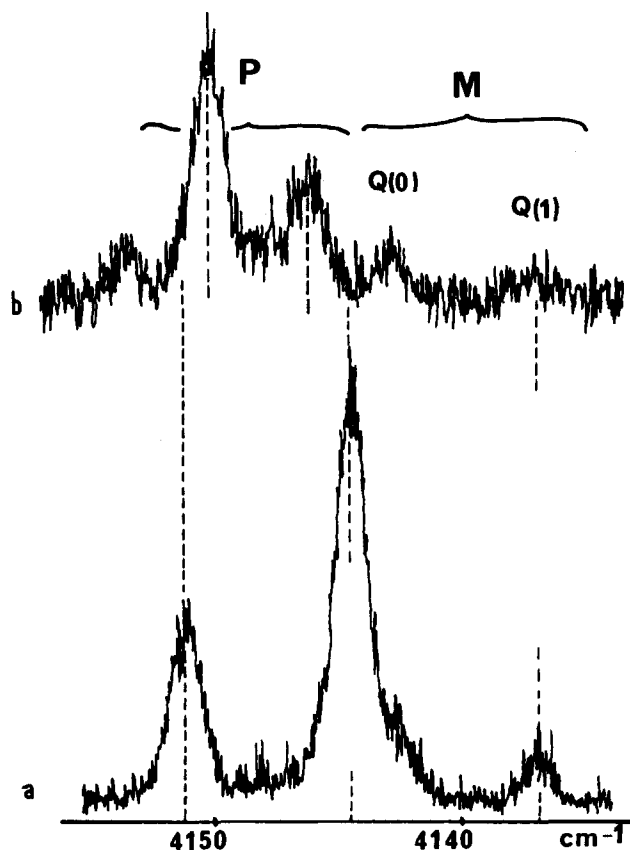


FIG. 6. Spectral changes in the vibrational region of H<sub>2</sub> trapped in solid Ar according to the ortho/para ratio ( $\rho_Q$ ). Spectra recorded at 10 K after annealing to 42 K. (a) H<sub>2</sub>/Ar = 3/100,  $\rho_Q = 2.2$ ; (b) H<sub>2</sub>/O<sub>2</sub>/Ar = 2/0.5/100,  $\rho_Q = 0.5$ . The  $\rho_Q$  values [ $\rho_Q = IQ(1)/IQ(0)$ ] were measured before annealing, i.e., before appearance of polymer lines.

As observed for H<sub>2</sub> and HD polymer bands, the *P* doublet experiences a large and reversible blue shift, of the order 0.15 cm<sup>-1</sup> K<sup>-1</sup>, upon increase of the recording temperature.

### Isotopic mixtures

About ten experiments were carried out with mixed samples in order to evidence vibrational couplings within aggregates. The frequency of each line was measured at least three times in order to ascertain small shifts with respect to the values obtained with only one isotopic species. The accuracy of the shifts is better than 0.2 cm<sup>-1</sup>. The most significant results obtained for HD and D<sub>2</sub> are reported below.

### Isotopically diluted HD

Table II presents the frequencies of the *P* and *P'* lines of HD diluted either in H<sub>2</sub> or D<sub>2</sub> with HD/H<sub>2</sub> or D<sub>2</sub> molar ratios equal to 0.68. *P'* was observed after a first annealing to 37–38 K while *P* was identified after cycling the matrix temperature to 40 K. These identifications were made unambiguous by the parallel observation of the corresponding lines of H<sub>2</sub> or D<sub>2</sub>. Both *P* and *P'* lines of HD are blue shifted upon isotopic dilution, but these shifts are more pronounced in HD/H<sub>2</sub> than in HD/D<sub>2</sub> mixtures (Table II). In all cases the linewidths remain narrow, of the order of 1.8 cm<sup>-1</sup> for spectral slit widths of 0.8 cm<sup>-1</sup>.

### Isotopically diluted D<sub>2</sub>

Four experiments were performed with D<sub>2</sub> diluted either by HD or by H<sub>2</sub>. The observations made on the *P* doublet after several annealing cycles to 40–42 K, independent of the dilutant, are twofold: on the one hand, both lines are blue shifted (Table II), on the other hand, their intensity ratio is inverted and roughly recovers the *Q*(0)/*Q*(1) monomer value. These results are clearly evidenced in Fig. 7 which compares the spectra obtained after successive annealings to 40 K for binary [D<sub>2</sub>/Ar = 3/100, Fig. 7(b)] and ternary [D<sub>2</sub>/H<sub>2</sub>/Ar = 0.8/4/100, Fig. 7(c)] mixtures.

TABLE I. Vibrational frequencies (cm<sup>-1</sup>) of natural H<sub>2</sub>, HD, and D<sub>2</sub> trapped in solid argon (recording temperature: 10 K). M: monomer. D: dimer, *P*, *P'*, *P''*: polymer lines observed after annealing.

	H <sub>2</sub>	HD	D <sub>2</sub>
<i>M</i>	4142.1	3615.4	2979.2
<i>D</i> <sup>a</sup>	4143.5	3616.0	
<i>Q</i> (0) <i>P'</i>	4152.7	3623.4	2986.9
<i>P</i>	4151.5	3622.0	2985.1
<i>P''</i>		3620.2	
<i>M</i>	4136.2		2977.0
<i>D</i> ( <sup>a</sup> )	4137.5		
<i>Q</i> (1) <i>P'</i>	4145.8		2984.9
<i>P</i>	4144.5		2983.1

<sup>a</sup> Position of the dimer line estimated from the frequency shift of the monomer line upon hydrogen concentration increase.

TABLE II. Vibrational frequencies ( $\text{cm}^{-1}$ ) of isotopically mixed hydrogen polymers  $P$  and  $P'$  in solid argon (in parentheses: frequency shifts with respect to pure species frequencies).

	HD in $\text{H}_2^a$	HD in $\text{D}_2^b$	$\text{D}_2$ in $\text{H}_2^c$	$\text{D}_2$ in HD <sup>b</sup>	$\text{H}_2$ in HD <sup>a</sup>
$P$	3624.0( + 2.0)	3623.1( + 1.1)	2986.5( + 1.4)	2986.2( + 1.1)	4151.8( + 0.3)
			2984.3( + 1.2)	2984.8( + 1.3)	4144.8( + 0.3)
$P'$	3625.1( + 1.7)	3624.4( + 1.0)			4151.1( + 0.4)
					4146.7( + 0.9)

<sup>a</sup> HD/ $\text{H}_2$ /Ar = 1.1/1.6/100.

<sup>b</sup> HD/ $\text{H}_2$ /Ar = 1.1/1.6/100.

<sup>c</sup>  $\text{D}_2$ / $\text{H}_2$ /Ar = 0.8/4.0/100.

## DISCUSSION

### Lower states of aggregation

Two parameters contribute to the aggregation processes in inert matrices: concentration and sample annealing. It appears that in the case of the trapping of hydrogen molecules their roles are remarkably different. On the one hand, the variation of the vibrational spectrum observed after deposition at 10 K with the hydrogen concentration is not very marked, although significant. Indeed, each  $Q(J)$  line experiences at most a  $2 \text{ cm}^{-1}$  blue shift. The shift clearly increases with hydrogen concentration. Assuming a random

trapping during deposition, the probability of formation of small aggregates (dimers, trimers) corresponding to the localization of several dopant molecules in nearest neighbor substitutional sites strongly increases when the hydrogen/argon molar ratio varies from 0.01 to 0.06. Accordingly, the blue shift of the monomer lines is attributed to line overlapping of monomers and low stoichiometry aggregates. Two observations corroborate this conclusion: (i) in krypton matrices the same phenomenon was observed but the extra blue shifted features (intensities of which increase with hydrogen concentration) are better resolved from the monomer lines (1); (ii) in the gas phase the vibrational frequencies of  $(\text{H}_2)_2$  and  $(\text{D}_2)_2$  are also identified very close to that of the monomer.<sup>5</sup>

### Higher states of aggregation

Sample annealing led to a totally different situation, with appearance of strongly blue shifted lines and concomitant disappearance of the lines located in the monomer region. Careful control of the annealing conditions together with a systematic study of the concentration dependence on the growth of these lines allowed two important observations: (i) the successive appearance of two larger aggregate features,  $P'$  and  $P$ ; (ii) there are minimal hydrogen/argon molar ratios for the appearance of species  $P'$  and  $P$ . Their values are 0.01 and 0.019, respectively, in our experimental conditions (10 K deposition temperature,  $\approx 30 \mu\text{mol/h}$  deposition rate and 40 K annealing temperatures).

Experiments using isotopic dilution and variable ortho/para ratios led to two important observations which demonstrate the existence of vibrational coupling between hydrogen oscillators belonging to the same aggregate:

(i) Upon isotopic dilution, one observes upward frequency shifts of the aggregate lines and, in the case of  $\text{D}_2$ , intensity inversion within the ortho/para doublets (see Fig. 7).

(ii) For  $\text{H}_2$ , there is a marked ortho/para ratio dependence on the frequencies as well as on the relative intensities of the two components of each of the  $P$  or  $P'$  doublets. Incidentally, this observation is similar to the one made for ortho/para mixtures of solid  $\text{H}_2$  and  $\text{D}_2$ ,<sup>4,5</sup> with, in particular, an intensity ratio between the low/high frequency components of the doublets greater than the population ratio of the  $J = 1$  and  $J = 0$  states (Fig. 8).

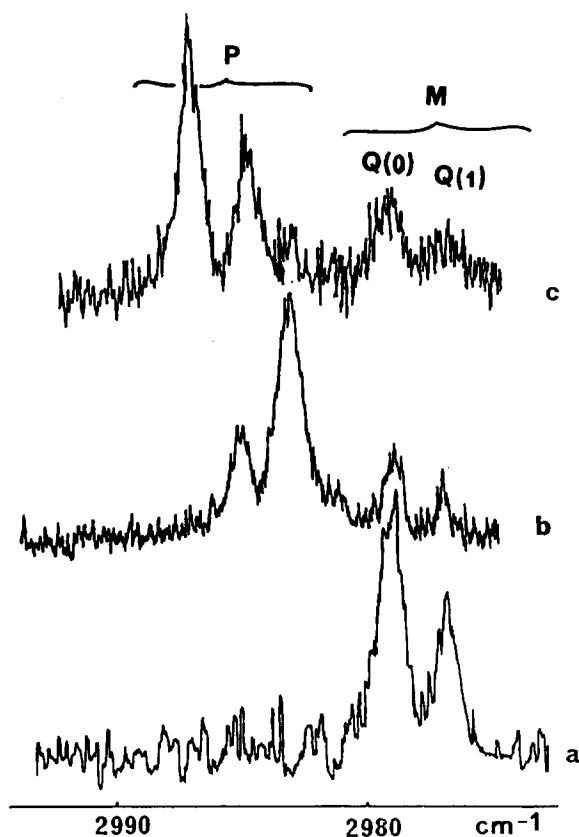


FIG. 7. Vibrational spectra of  $\text{D}_2$  trapped in solid argon, recorded at  $T_r = 10 \text{ K}$ . (a) after deposition at 10 K for  $\text{D}_2/\text{Ar} = 2/100$ ; (b) same sample as (a), recorded after annealing to 40 K; (c) after annealing to 40 K for  $\text{D}_2/\text{H}_2/\text{Ar} = 1/2.2/100$ .

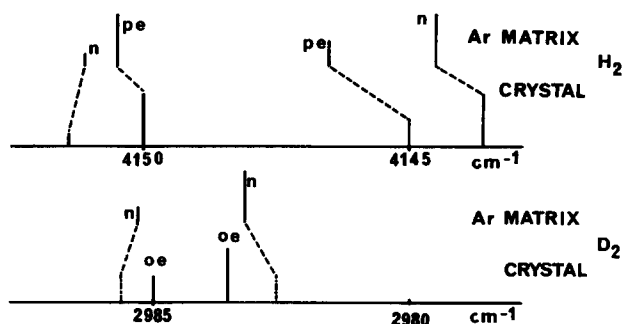


FIG. 8. Comparison between the Raman spectra of solid  $\text{H}_2$  and  $\text{D}_2$  at 2 K (Refs. 3, 4) and those of aggregates  $P$  trapped in solid Ar at 10 K.  $n$ : natural sample;  $pe$ : para enriched  $\text{H}_2$  ( $p/o = 5.6$ );  $oe$ : ortho enriched  $\text{D}_2$  ( $o/p = 4$ ). The length of the bars is proportional to the intensity of the observed bands except for natural  $\text{D}_2$  bands in the solid state whose spectra were not reported in Ref. 3.

To account for these data, we have undertaken force field calculations, assuming that each aggregate has the most closely packed structure possible. The following model was considered in order to simulate the vibrational spectrum:

(i) Molecules are classified into two kinds of oscillators, ortho or para, each kind being characterized by slightly different reduced reciprocal masses,  $G_o$  and  $G_p$ , with  $G_o/G_p = (\nu_o/\nu_p)^2$ .

(ii) The coupling between oscillators is introduced through interaction force constants  $f$  which are defined as the second derivative of the intermolecular  $\text{H}_2\text{--H}_2$  pair potential. As discussed by Van Kranendonk *et al.*,<sup>6,7</sup> the main contribution should arise from the attractive dispersion potential. As a consequence  $f$  has a negative value, with a  $R^{-6}$  dependence (where  $R$  is the intermolecular distance).

(iii) In the calculations of the Raman band intensities the polarizability anisotropy is neglected. This simplification stems from the low value of the depolarization ratio of the  $Q$  branch ( $\rho \approx 0.01^8$ ).

Calculations were performed for both isotopically pure and isotopically mixed polymers. In the first case states of aggregation varying from 2 to 6 were examined. For  $n = 2, 3, 4$  all the molecules are in nearest neighbor positions, which means that the interaction force constants  $f$  are the same whatever is the pair considered. Because of the equivalence between the molecules the number of aggregates including all the possibilities of ortho/para substitution is equal to  $(n + 1)$ . For  $n = 5$ , close packing implies a  $D_{3h}$  structure with two nonequivalent positions, axial and equatorial; therefore, two different interaction force constants have to be introduced: one  $f_{nn}$  between nearest neighbors (equatorial–equatorial and axial–equatorial molecules), the other  $f_{nnn}$  relating to the axial–axial interaction. Since the axial–axial distance is  $\sqrt{2}$  times greater than the distance between nearest neighbors,  $f_{nnn}$  is expected to be eight times smaller than  $f_{nn}$ . Twelve different ortho/para mixed species have to be considered in the calculations. For  $n = 6$  the structure is that of an octahedron, all the molecules being equivalent. Two interaction force constants are introduced,  $f_{nn}$  and  $f_{nnn}$ ,

with  $f_{nn} \approx 8f_{nnn}$ . The number of mixed ortho/para aggregates is also equal to 12.

Band intensities were deduced from the knowledge of the eigenvectors and of the relative abundances of the ortho/para mixed species. Starting from the expression of the isotopic Raman band intensities for the  $m$ th mode of species  $\mu$ :

$$I_m^\mu = K \left( \frac{\partial \bar{\alpha}}{\partial Q_m^\mu} \right)^2 N_\mu,$$

where  $Q_m^\mu$  is the normal coordinate associated to this mode and  $N_\mu$  the relative abundance of species  $\mu$ , one may write

$$I_m^\mu = K \left( \sum_i \frac{\partial \bar{\alpha}}{\partial r_i} \frac{\partial r_i}{\partial Q_m^\mu} \right)^2 N_\mu, \quad (1)$$

where  $r_i$  is the stretching coordinate of the  $i$ th molecule of the aggregate. Since  $\partial \bar{\alpha} / \partial r_i$  is the same for each molecule, Eq. (1) becomes

$$I_m^\mu = K \left( \frac{\partial \bar{\alpha}}{\partial r} \right)^2 \left( \sum_i \frac{\partial r_i}{\partial Q_m^\mu} \right)^2 N_\mu. \quad (2)$$

$I_m^\mu$  appears to be proportional to the square of the sum of the components of the eigenvector weighted by the relative population of the species. This relative population is calculated from the ortho/para molar ratio deducible from the relative intensities of the monomer lines, and assuming a random distribution of ortho/para states within the aggregates (binomial distribution). A synthetic spectrum was drawn by coadding the contributions of all the species, assuming Gaussian band profiles, with FWHM equal to the spectral slit width—it was observed that the monomer band profile is roughly Gaussian, with FWHM close to the apparatus function (see Figs. 9, 10).

Calculations were performed for the three isotopic species, starting from reasonable values of the force constants, that producing splittings between the ortho/para frequencies of  $6.0 \pm 0.5$  and  $2.0 \pm 0.3 \text{ cm}^{-1}$  for  $\text{H}_2$  and  $\text{D}_2$ , respectively, and a coupling shift of  $0.4 \pm 0.2 \text{ cm}^{-1}$  between  $\text{H}_2\text{--H}_2$  nearest neighbors (to be compared to  $0.49 \text{ cm}^{-1}$  in the crystal.<sup>6</sup>). Adjustment of the force constants was performed separately for each isotopic species in order to avoid corrections stemming from anharmonicity and from slight changes induced by variations in zero point energy from one isotopic aggregate to the other.<sup>8</sup>

Calculations performed on  $(\text{HD})_n$  are not significant since, whatever the value of  $n$ , only the totally symmetrical mode is Raman active. Note that this in-phase mode has the lowest frequency, because of the negative value of the interaction force constant. This assertion rigorously holds for  $n = 2, 3, 4, 6$ ; for  $n = 5$ , because of the nonequivalence between axial and equatorial molecules, two vibrations are in principle Raman active, but the higher frequency one is 3 orders of magnitude less intense than the low frequency, totally symmetrical mode. For  $\text{H}_2$  and  $\text{D}_2$  the synthetic spectra account semiquantitatively for the experimental data. Each spectrum displays two components whose splitting and relative intensity ratio obey the following rules:

(i) The low frequency component is always stronger than expected based only on the ortho/para relative abundance.

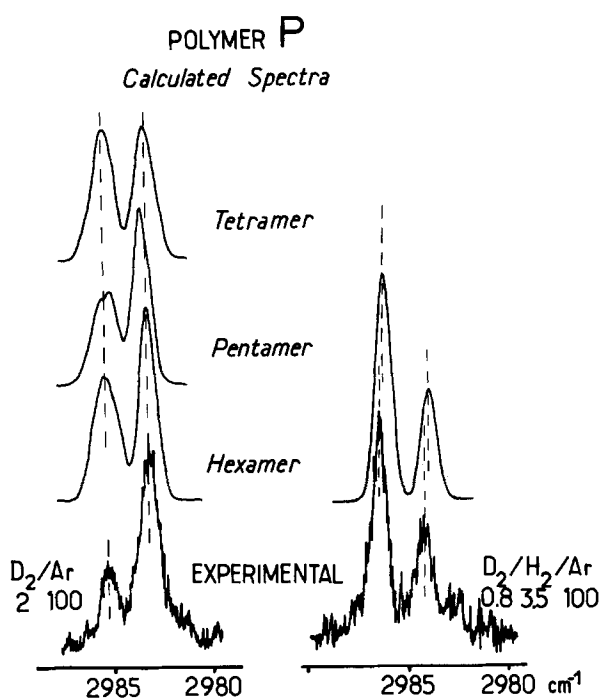


FIG. 9. Comparison between experimental and calculated spectra for aggregate species  $P$  in the pure  $D_2$  case (ortho/para ratio  $\rho = 3$ ) and in the case of  $D_2$  diluted by  $H_2$  ( $\rho = 2$ ). The synthetic spectra are calculated using Gaussian band profiles for each individual component, weighed by their statistical probability and finally, renormalization to the most intense experimental signal. The frequencies are calculated using the following parameters (in  $cm^{-1}$ ):  $\nu_o = 2986.2$ ,  $\nu_p = 2983.9$  are the positions of isolated ortho and para  $D_2$  molecules. The vibrational coupling constants are (in  $cm^{-1}$ ):  $-0.38$  between nearest neighbors and  $-0.055$  between non nearest neighbors.

(ii) For  $H_2$  the splitting is all the smaller as the para abundance is greater.

Both rules, which also hold for solid hydrogen,<sup>4</sup> are well explained by the existence of vibrational coupling between molecules within the aggregates, which enhances the Raman intensity of the low frequency (totally symmetric) modes. As a consequence, in the case of  $D_2$  where the ortho-para vibrational coupling is strong because of the small ortho/para splitting ( $2\text{ cm}^{-1}$ ), the low frequency component is three times stronger than the high frequency one, while, in absence of coupling, this low frequency component would have been at least twice as weak as the other (Fig. 9). On the other hand in the case of  $H_2$  where the ortho-para coupling is weaker because the ortho/para splitting is greater ( $\approx 6\text{ cm}^{-1}$ ), only the ortho molecules remain significantly coupled together in a normal situation (where para molecules are statistically much more likely to be surrounded by ortho than by para molecules). As a consequence the ortho signal is lowered with respect to what would be expected in absence of coupling and the para-ortho splitting is large (of the order of  $7\text{ cm}^{-1}$ ); in case of ortho  $\rightarrow$  para conversion, the proportion of aggregates with large numbers of para molecules is greater, the para molecules are then coupled together and the corresponding signal is globally red shifted. Since the

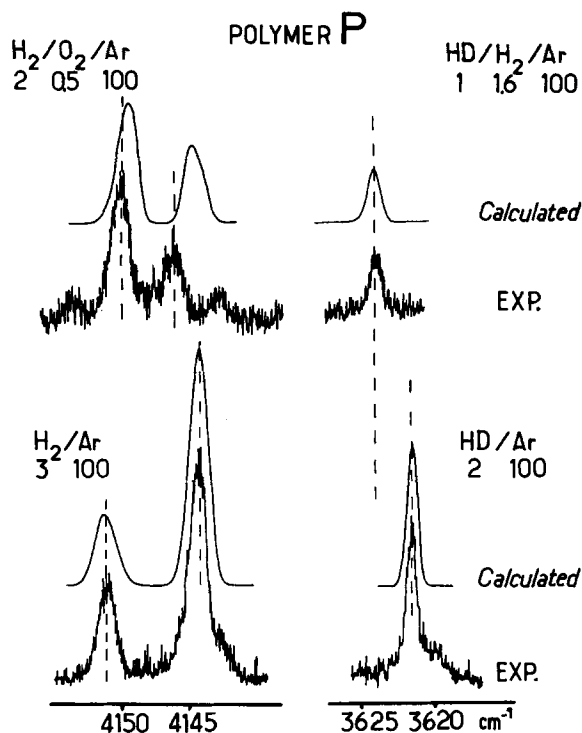


FIG. 10. Comparison between experimental and calculated spectra in the pure  $H_2$  or  $HD$  case and in the case of para-enriched  $D_2$  or  $HD$  diluted in  $H_2$ . Synthetic spectra calculated using Gaussian band profile. The frequencies are calculated using the following parameters (in  $cm^{-1}$ ):  $\nu_o(H_2) = 4146.0$ ,  $\nu_p(H_2) = 4152.0$ . The vibrational coupling constants are (in  $cm^{-1}$ ):  $-0.38$  between nearest neighbors and  $-0.055$  between nonnearest neighbors. The ortho/para ratio  $= 1.5$  (bottom trace, in absence of oxygen) and  $0.25$  (top trace).

ortho molecules are now mostly uncoupled the lower frequency signal is shifted upward, and both effects decrease the para-ortho splitting down to  $4/5\text{ cm}^{-1}$  (see Fig. 10, left traces).

Calculations were also performed for isotopically mixed aggregates. The spectral simulation is simple for diluted  $HD$  whatever the degree of aggregation  $n$  assumed ( $2 \leq n \leq 6$ ). The molar fractions of each isotopic species determine the probability of finding mixed aggregates of the type  $(HD)_x(X_2)_{n-x}$  ( $X = H$  or  $D$ ) and the spectra of the  $(HD)_x$  aggregates are calculated, taking into account all the structural possibilities. The synthetic spectrum obtained for hexameric  $HD/H_2$  mixed species with  $HD/H_2$  molar ratio of  $0.3$  displays a slightly broadened  $Q(0)$   $HD$  band,  $2\text{ cm}^{-1}$  blue shifted with respect to pure  $HD$ , in rather good agreement with the observed spectrum (Fig. 10, right traces).

Finally, all these calculations reproduce semiquantitatively the various experimental data described above. It is also possible to establish with certainty that the spectral properties of species  $P$  cannot be satisfactorily reproduced using models involving less than six molecules. This corroborates the indication given by the concentration studies that the  $P$  lines have at least an eight order dependence with respect to the hydrogen concentration. Figure 9 presents comparison



between experimental data and the best simulated spectra for  $(D_2)_n$  and  $(D_2)(H_2)_{n-1}$  close packed aggregates.  $D_2$  constitutes the best test of the model owing to the stronger coupling between ortho and para molecules. It is clear that tetra or pentamer models are less satisfying than hexamer models. Nevertheless even the hexameric model is unable to reproduce correctly the intensity ratio between the two components of the  $(D_2)_n$  species doublet. We think that this indicates that  $n > 6$  and, in our opinion, does not allow to conclude about the exact state of aggregation. In other words, the spectral changes arising from vibrational couplings within (hydrogen) $_n$  aggregates for  $n$  varying from six to infinity are too small and difficult to analyze owing to the fact that accurate force field calculations are not tractable for  $n$  greater than six.

The discussion on the size of aggregates, not possible on the basis of vibrational couplings, has to take into account three remarkable properties of the  $P$  and  $P'$  lines: (i) Their positions, notably blue shifted with respect to those of the monomer and of the low aggregate signals, (ii) their nearly complete invariance with respect to changes of host crystal, and (iii) the large temperature dependence of their frequencies. Observations (i) and (ii) tend to prove that these aggregates have vibrational properties closer to that of the pure crystal than to small, weakly bonded species sensitive to hydrogen-matrix as well as to hydrogen-hydrogen interactions. For example, for  $H_2$  trapped either in argon or in krypton, the monomer lines experience a  $10\text{ cm}^{-1}$  red shift while the  $P$  lines are  $2\text{ cm}^{-1}$  blue shifted from Ar to Kr matrices.<sup>9</sup> Hence, the attractive contribution of the Ar or Kr- $H_2$  pair potential does not play any significant role on the vibrational response of the aggregates. This is a strong indication that a direct interaction between matrix host atoms and molecules within the aggregate is less important than molecule-molecule interactions. These observations are best explained considering the aggregates as microcrystals of a size such as surface molecules will be much less abundant than inner or bulk molecules. Corresponding spectra are thus expected to be close to that of the crystal, which is quite well verified according to the results obtained by Welsh's group. On the one hand, in the case of HD the positions of the  $P$  line ( $3622.0\text{ cm}^{-1}$ ) and that of the  $Q(0)$  line of the crystal ( $3621.85\text{ cm}^{-1}$ ) agree remarkably well. On the other hand, for the symmetrical species, small differences are observed (Fig. 8), in particular for the low frequency  $P$  component of  $H_2$  which is blue shifted by about  $1\text{ cm}^{-1}$  from the crystal to the matrix. But the relative intensities of the low/high frequency components for the crystal bands and the  $P$  doublets agree quite well. These small differences could be tied to changes either in temperature (crystal at 2 K, matrix at 10 K) or in the internal pressure within microcrystals. Both changes would lead to frequency increase from the crystal to

the matrix. Indeed we have observed a frequency increase of the  $P$  lines with temperature; furthermore it is well known<sup>10</sup> that pressure effects on the  $H_2$  crystal induce blue shifts for the vibrational lines of the order of  $2\text{ cm}^{-1}/\text{kbar}$ .

## CONCLUSION

From the Raman data analysis it appears that aggregation of hydrogen in solid argon does not proceed as usually observed for heavier diatomic or polyatomic molecules. Instead of successive appearances of bands typical of multimers of increasing size for increasing values of annealing temperature and/or annealing duration, hydrogen molecules are found to be clustered in microcrystals as soon as their migration within the rare gas crystal is temperature allowed. The size of the microcrystals is difficult to determine since force field calculations only lead to a semiquantitative description of the spectra. However several observations suggest that it should be quite large: (i) The polymer line frequencies are weakly matrix dependent, in opposition to observations made for  $Q(J)$  lines of monomeric and dimeric species. Thus the number of surface molecules, sensitive to the matrix environment, should be small compared to the one relating to bulk molecules. (ii) Most of the spectral properties are close to those observed for the crystal. Such an aggregation process is comparable to separation of the dopant from the host crystal, an expected phenomenon if one keeps in mind the low solubility of  $H_2$  in solid Ar. Welsh and co-workers<sup>11</sup> have reported the difficulties they had to overcome for obtaining solid  $H_2$  doped argon for IR absorption experiments. They mentioned that the liquid to solid phase transition easily led to bubble formation because of the low  $H_2$  solubility in the solid phase. We feel that the same process occurs upon annealing; the  $H_2$  concentration in our experiments is much greater than its solubility so that temperature increase leads to phase separation.

<sup>1</sup>M. E. Alikhani, B. Silvi, J. P. Perchard, and V. Chandrasekharan, *J. Chem. Phys.* **90**, 5221 (1989).

<sup>2</sup>F. T. Prochaska and L. Andrews, *J. Chem. Phys.* **67**, 1140 (1977).

<sup>3</sup>S. S. Bhatnagar, E. J. Allin, and H. L. Welsh, *Can. J. Phys.* **40**, 9 (1962).

<sup>4</sup>V. Soots, E. J. Allin, and H. L. Welsh, *Can. J. Phys.* **43**, 1985 (1965).

<sup>5</sup>A. R. W. McKellar and H. L. Welsh, *Can. J. Phys.* **52**, 1082 (1974).

<sup>6</sup>J. Van Kranendonk, *Physica* **25**, 1080 (1959); *Can. J. Phys.* **38**, 240 (1960).

<sup>7</sup>J. Van Kranendonk and G. Karl, *Rev. Mod. Phys.* **40**, 531 (1968).

<sup>8</sup>W. Holzer, Y. LeDuff, and K. Altmann, *J. Chem. Phys.* **58**, 642 (1973).

<sup>9</sup>M. E. Alikhani, L. Manceron, and J. P. Perchard, *Chem. Phys.* (in press).

<sup>10</sup>M. Jean-Louis, M. M. Thiery, H. Vu, and B. Vodar, *J. Chem. Phys.* **55**, 4657 (1971).

<sup>11</sup>R. J. Krieglner and H. L. Welsh, *Can. J. Phys.* **46**, 1181 (1968).